Anal. Chem. **2002,** *74,* 4361−4369

Semiautomated Analytical Image Correlation

T. Gregory Schaaff, J. M. McMahon, and Peter J. Todd*

Chemical Sciences Division, Oak Ridge National Laboratory, Bldg. 5510-MS-6365, Oak Ridge Tennessee 37831-6365

Machine vision refers to computer programs consisting of a collection of pattern recognition and digital image processing algorithms (Fabel, G. *Motion Control* 2000, 53−54). A version of machine vision has been applied to correlating digital images generated by optical microscopy and secondary ion mass spectrometry (SIMS). By suitable application of image processing algorithms, semiautomated correlation between optical and secondary ion images is possible. For correlation of minor constituents evident in secondary ion images but invisible in optical images, correlation is performed by reference to the relative position of minor to major constituents. Precise coordinates of features apparent in one analytical image can be translated into the corresponding coordinates of an analytical image obtained by a different method. In principle, this capability yields a semiautomated system to combine complementary features of disparate imaging methods, such as secondary ion and optical microscopy.

Machine vision systems are increasingly used to monitor automated manufacturing processes.[1] High-speed computers integrated with video cameras use machine vision programs to provide "visual feedback" to robotic devices so that parts can be inspected and appropriately oriented before and after each successive operation. The geometry of viewing can be widely different, depending upon the environment of a particular stage of manufacture, and the programs are used to integrate the successive machine vision/robot systems as manufacturing proceeds. At one stage of manufacture, the video camera might be located a few centimeters from the part in question, and at the next stage, the camera might be one meter or more from the part and view it from a different perspective or under different lighting conditions. "Eye−hand coordination" between camera and robotic arm is essential, but machine vision programs must also recognize flawed parts and possibly incorrect parts. Thus, machine vision algorithms must calibrate and correlate images obtained under a variety of circumstances and, to be useful, must perform these operations quickly. In fact, machine vision works well in manufacturing.

Problems similar to those of automated manufacture arise when large numbers of samples are mapped and imaged by disparate analytical imaging methods. Methods of interest include optical microscopy, scanning and transmission electron microscopy (SEM and TEM, respectively)[2], secondary ion mass spectrometry/microscopy (SIMS),[3] and a variety of scanning probe microscopic (SPM) techniques.[4] With these disparate methods, not only component (i.e., sample) orientation but also instrument geometry and the analytical signal specific to each imaging method must be considered in correlating images. In fact, extraction of chemical information is severely hindered by the inability to directly compare distributional information obtained by complementary methods. For example, secondary ion images can provide a wealth of elemental and molecular information concerning samples;[3] however, manual correlation of secondary ion micrographs with other types of micrographs can be difficult. Intensity variations evident in the secondary ion micrograph of a sample may not have corresponding variations evident in images produced by optical or electron microscopy.[4] Some elements evident in an optical micrograph do not yield abundant secondary ions, and of course, some trace components, such as Na, are invisible in an optical image but yield abundant secondary ions. Notwithstanding these pitfalls, there are likely far more sample types wherein some similarity in images produced by different methods permits correlation.

There are many types of samples for which mapping by complementary analytical methods is required,[5] and some of these samples fall within the statutory mission of the U. S. Department of Energy to develop methods for analysis and correlation. Such correlation is currently done manually. As a consequence of evolution, human beings are quite able to rapidly assimilate vast quantities of information via images, and humans are thus capable of timely image correlation. It is by no means obvious that computers can perform such correlation in a timely manner, because they must acquire image data one byte at a time. However, image correlation quickly becomes a tedious and stressful process to humans, and performance can be quite variable.[6] Computer assistance in the effort is thus worth investigating. We hypothesized that machine vision algorithms, if integrated with an appropriate main program, could perform analytical image correlation faster than humans alone, with greater consistency and at a lower cost, particularly if some human judgment and knowledge of the sample could be used to complement the algorithms.

* To whom correspondence should be addressed. Phone: 865-574-6824. E-mail: toddpj@ornl.gov.

(1) Fabel, G. *Motion Control* **2000**, 53−54.
(2) Goldstein, J. I.; Newbury, D. E.; Echlin, P.; Joy, D. C.; Romig, A. D. J.; Lyman, C. E.; Fiori, C.; Lifshin, E. *Scanning Electron Microscopy and X-ray Microanalysis: A Text for Biologists, Materials Scientists, and Geologists*, 2nd ed.; Plenum Press: New York, 1992.
(3) Benninghoven, A. *Secondary Ion Mass Spectrometry Basic Concepts, Instrumental Aspects, Applications and Trends*; Wiley-Interscience: New York, 1987.
(4) Thornton, J. T. *Surf. Eng.* **2000**, *16*, 287−293.
(5) Morrison, G. H.; Gay, I.; Chandra, S. *Scanning Microsc. Suppl.* **1994,** *8*, 359−70.
(6) Albert, M. K.; Hoffman, D. D. *Perception* **2000,** *29*, 303−12.

10.1021/ac025693b CCC: $22.00
Published on Web 07/26/2002

Automated image correlation, even with images obtained from the same platform, is not a straightforward problem. With optical microscopy, for example, subtle changes in magnification, focus, position or illumination can cause identical samples to appear completely different. This kind of problem arises when samples arrive for a type of analysis, along with a suite of images purporting to describe the sample. As with manufacturing, intensity normalization and geometric conversion must be performed before any correlation is attempted.

Correlation becomes complex when the orientation and spatial resolution of reference and test images are different. Fiducial or reference marks can be used in some respects to mitigate this problem, but adding fiducials to a chemical sample mount adds yet another sample handling step, requires that the sample and fiducial be in the same field of view, and will almost certainly be different from operator to operator.

An even more complex problem exists when images are derived from different imaging platforms. The most obvious problems in correlating secondary ion micrographs to optical micrographs arise from the different fields of view and geometries unique to each system. In most cases, the mean axis of the primary ion beam of an ion microprobe is not normal to the sample surface; however, the mean optical axis of microscopes is normal to the sample surface. These differences in mean imaging axes cause discrepancies in coordinate systems of images from the same sample. Although a different domain, these are exactly the problems that machine vision algorithms were developed to solve. The advantage that the analyst has over a robot is that for the most part, the geometric particulars of each analytical platform are reasonably well-known and can be corrected by simple matrix operations.

In this paper, we describe the operation and performance of a commercially available collection of image operation and pattern recognition algorithms we have integrated into a program we call SIMSearch 0.9b. We evaluate the program's ability to correlate optical images with each other and with secondary ion images. We also evaluate the program to find correlations that enable use of surrogate objects evident in secondary ion images to find an object not evident or distinguishable in optical images of the same sample.

EXPERIMENTAL SECTION

Secondary Ion Mass Spectrometry/Microscopy. Mass-selected secondary ion images were obtained using a custom-built wide-field-of-view magnetic sector ion microprobe with Mattauch−Hertzog geometry.[7,8] The mass analyzer is a modified JEOL JMS-01 μ_B-2 double-focusing mass spectrometer equipped with electronic pulse counting detection. The primary ion beam (15 keV) is generated from a gallium liquid metal ion gun (FEI Corporation) that in its present configuration produces a primary ion beam spot size of 1 μm. Typically, 200 × 200 and 500 × 500 pixel images were acquired by rastering the primary ion beam over a specified area of 0.1−1 cm^2 and monitoring the intensity of secondary ions of interest emitted from the surface. The samples used in these initial studies were prepared by dispersing metallic particles on silver paint, followed by low-temperature ashing (ozone plasma etching) to enhance the secondary ion yield. Manganese flakes (∼150 μm), titanium spheres (∼75−100 μm) (Alpha Aesar, Ward Hill, MA), and palladium spheres (75−100 μm) (Phrasor Scientific, Duarte, CA) were used for sample preparation.

Optical Microscopy. The optical microscopy equipment included (a) an optical microscope (Infinivar, Infinity Inc.), (b) a CCD camera (Sony XC-75) to capture 640 × 480 gray-scale images, (c) a separate camera monitor (Sony), and (d) a PCVision Frame grabber (Imaging Technology Inc.). The computer used for image processing and image correlation was a 566 MHz Pentium III with 128 MB RAM (X-Technology) and a 32 MB (SDRAM) video card (Diamond Stealth). SIMSearch was written in Visual Basic 6 to run under both Windows 98 and NT environments. Source code can be obtained gratis from the authors.

Subroutine libraries and frame grabber drivers from Imaging Technology, Inc.(ITI) (www.imaging.com) necessary to integrate the system, develop the software for SIMSearch, and to use SIMSearch were purchased for about $4000. Importantly, the ITI frame grabber need not be connected to any camera, but must be installed on the computer using the image processing libraries, since a number of processing functions are performed using the memory of this frame grabber. All images used for correlation were 8-bit gray-scale bitmap images, that is, intensity-measured and displayed in 256 shades of gray.[9]

RESULTS AND DISCUSSION

Application of Pattern Recognition Methods. Analytical images are generally digital matrix representations of some type of measurable unit, such as intensity or abundance. Mathematically, $I = f(r, c)$, where I is intensity, and r and c are the row and column number, respectively, corresponding to a place on the sample. In optical microscopy, for example, intensity $I(x, y)$ is optical density at the point (x, y) on the sample and represented in an image as $\mathbf{G} = f(r, c)$.[10] The connection between (x, y) on the sample and (r, c) in the presented image is determined by the field of view of the microscope employed and the array size (number of pixels) of the presented image. Indexing of row and column begins at the upper left corner of the image; x coordinates increase from left to right, and y coordinates increase from top to bottom. To simplify discussions, we use the same scheme when referring to the sample.

The first step of pattern recognition is normalization. For a gray-scale bitmap image, any element of $\mathbf{G}$ can have integer values anywhere between 0 and 255.[9] To normalize intensity in an image, a new array can readily be generated by the operation of all values of r and c.

$$\mathbf{G}(r, c) = \mathbf{I}_{\text{normalized}}(r, c) = 255\{[I(r, c) - I_{\min}]/(I_{\max} - I_{\min})\} \quad (1)$$

Here, $\mathbf{I}_{\text{normalized}}$ refers to an array of normalized intensity at any

(7) Grimm, C. C.; Short, R. T.; Todd, P. J. *J. Am. Soc. Mass Spectrom.* **1991,** *2*, 362.

(8) Short, R. T.; Wiedenbeck, M.; Guo, X. Q.; McMahon, J. M.; Riciputi, L. R.; Todd, P. J. In *Secondary Ion Mass Spectrometry − SIMS XI*; Gillen, G., Lareau, R., Bennett, J., Dtevie, F., Eds.; John Wiley & Sons: Orlando, FL, 1998; pp 831−834.

(9) Adams, L. *Visualization and Virtual Reality;* Windcrest/McGraw-Hill: NewYork 1994.

(10) Andrews, H. C. *Introduction to Mathematical Techniques in Pattern Recognition*; Robert E. Krieger: Malabar, FL, 1983.

pixel specified by r row and c column in the image; I_{min} and I_{max} reflect the corresponding limits of intensity presented in the image.

Libraries of pattern recognition and machine vision functions, commercially available from a variety of sources, are convenient to use for prototype program development. Our purpose in using a commercial library of such functions has been to expedite determining whether cross platform analytical image correlation could be performed via personal computer in a timely and reliable manner. Nonetheless, mathematical pattern recognition is not a "black box" of proprietary methods. Although a complete description of pattern recognition methods is beyond the scope of this paper, a brief summary of elementary operations is essential to understanding the logic of analytical image correlation.[10]

Pattern recognition methods first involve defining three "spaces" or arrays of data. These are pattern space, (**P**), feature space (**F**), and classification space (**C**). For our purposes, pattern space is the analytical image in bitmapped format, representing normalized intensity (optical density or ion abundance) that is to be correlated with a reference analytical image. Feature space is defined, in general, as a unique set of features used for comparison with subsets in a pattern space. For our purposes, **F** is a selected portion of a reference image having a range of intensities and indicated by a "window" overlaid on the reference image. Classification space consists of the result of a set of operations or algorithms used for comparison of corresponding normalized intensities in both **F** and **P** or a subset of pattern space. **C** contains two vectors: (1) the offset (r, c) of the center of **F** from the origin of a reference image, and (2) the offset (r, c) of the center of the corresponding subset of **P** (which we call **P′**) that matches best with **F**. For instance, suppose there is an exact match between a window selected from a reference image, **F**, and a corresponding window in an image to be correlated (**P′**). The classification space **C** would then consist of the two sets of row and column indices specifying the centers of both windows in their respective images.

Highly efficient proprietary algorithms have been developed for classification; to be efficient, they must be simple. For example, the "distance" between two points in multidimensional space is the root-mean-square difference (RMS) between the coordinates of the two points. In pattern recognition, this is the difference between corresponding intensities in the feature space, **F**(r, c) and subsets of the pattern space **P**(r, c).

$$\mathbf{C}(r_i, c_j) = [\sum_{i,j} (\mathbf{F}(r, c) - \mathrm{P}'(r_i, c_j))^2]^{1/2} \qquad (2)$$

In Equation 2, the defined feature space (subset from the reference image, **F**(r, c)) is compared to a subset of pattern space, (**P′**(r_i, c_i)) having the same internal indices. The feature space is "stepped" through the pattern space at different (r_i, c_j) values, and at each step, the RMS difference for all intensities of the two subsets is determined. The best match between the feature space and the subset in the pattern space is found at the **C**(r_i, c_j) location that has the minimum value. Some features of this pattern recognition algorithm are shown in Figure 1.

In the context of analytical imaging, pattern recognition is completely separate from digital image processing, but the utility of pattern recognition depends heavily on the type and extent of well-characterized image processing performed. Changes to an image caused by rotation, lighting, focusing, etc., can reduce or

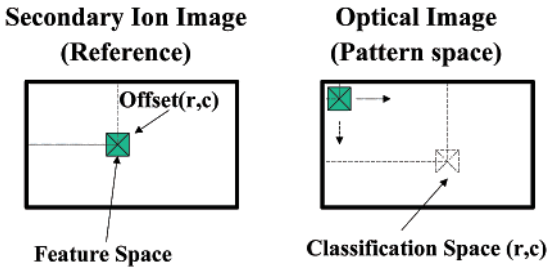

Figure 1. Schematic diagram of pattern recognition terms and algorithms.

enhance the effectiveness of pattern recognition methods. Thus, image artifacts must be corrected by digital image processing before any hope of correlation can logically exist. Such processing can range from simple linear transformation (e.g., rotation or magnification) to fairly complex distortions (e.g., differentiation in one or two dimensions). To both simplify discussion and illustrate the logical application of these methods, we have limited our use of digital processing to (a) brightness control, including threshold operations; (b) magnification; and (c) rotation. In normal operation, pattern recognition correlation would be attempted after each digital image process.

For the purpose of this report, we manufactured a sample appropriate for analysis by both SIMS and optical microscopy; we use different images of the same sample to demonstrate features of machine vision. Specifically, five Pd (75−100-μm diam) spheres were positioned approximately equidistant in a straight line on a copper slide coated with Ag paint. Subsequently, Ti spheres (75−100-μm diam) and Mn flakes were dispersed over a sample area of ∼1 cm diam. The Ti and Pd spheres are indistinguishable by optical microscopy, but the Mn flakes are irregular in shape and size. Thus, it is quite possible to specify the location of any sphere by its position relative to one or more of irregular Mn flakes.

Optical-to-Optical Correlation. Optical-to-optical image correlation demonstrates operations used by SIMSearch and provides familiarity with the terminology. The first test of the program was thus to correlate nearly identical optical images. This required first obtaining an optical image of the sample on the microscope stage and then storing the image as a bitmap file; i.e., this first image was taken to be the reference image. A second image was then obtained after (a) moving and rotating the sample but keeping it within the field of view of the microscope, (b) randomly changing illumination to the sample, and (c) changing the magnification slightly and refocusing the microscope. It is known that the effect of these operations on the resultant image can be corrected or "undone" by simple linear transforms (e.g., magnification, displacement, or rotation) or by simple digital image processing (focusing or lighting). Figure 2a shows the optical image obtained from the test sample, and Figure 2b shows the image at a slightly different magnification and with some rotation of the sample. Casual inspection of the two images conveys the difficulty in manual correlation, especially if it is not known that the two images were obtained from the same sample.

After capturing the optical image, the brightness of the captured optical image was adjusted "by eye" so that the apparent brightness of the reference and captured optical image were approximately equal. This is a relatively easy task, since exact

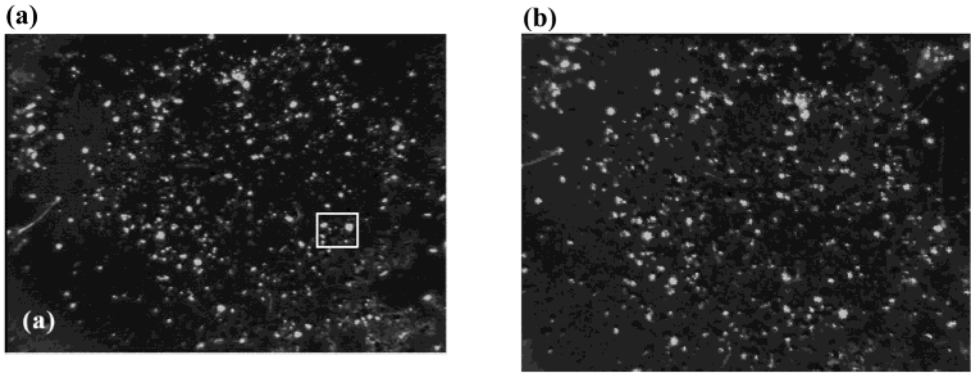

Figure 2. Optical images of Pd and Ti balls and Mn flakes dispersed on a Ag target. (a) The outlined box is the pattern defined for searching. (b) The same sample after the camera has been shifted and is operating at a different magnification. Although these two images can be readily correlated manually, the task quickly becomes tedious when more than two images are involved and becomes stressful when there is no guarantee that the images should correlate at all.

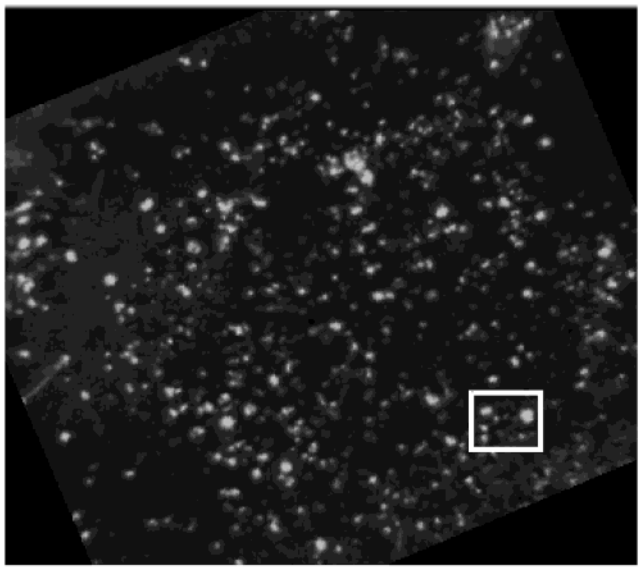

Figure 3. The rotation/scaling search function searches for the defined pattern (Figure 2a) after capturing an image and performing geometric and processing manipulations. The pattern match corresponding to the best fit with the defined pattern is outlined.

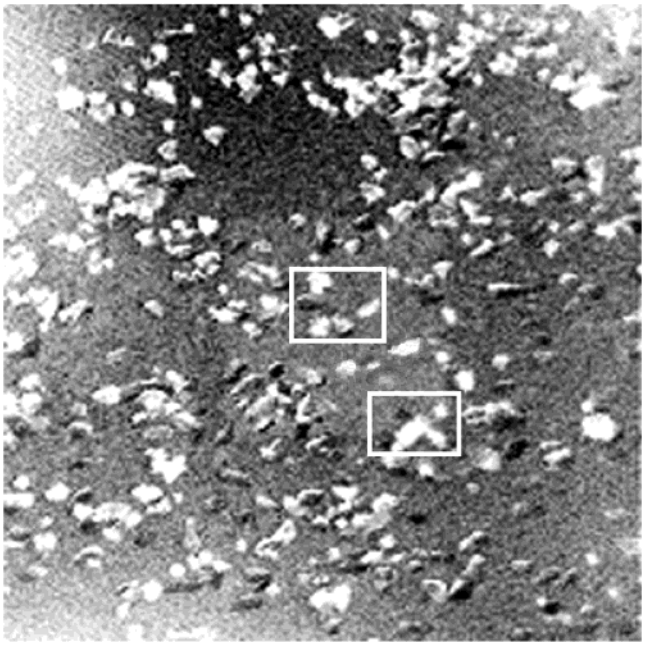

Figure 4. Secondary ion image (*m*/*z* 107, Ag) of sample shown in Figures 2 and 3. The ion intensity has been inverted; i.e., high *m*/*z* 107 intensity is dark, and low intensity, bright. Two patterns are defined above and outlined with white boxes.

correlation is not necessary to establish that two images are about the same brightness. A pattern or set of patterns was then defined in the reference image. The small white box shown in Figure 2a represents the defined feature space. This feature space was chosen for its unique lack of symmetry. We have found that in a field of dispersed particles, irregularity of a single particle's shape is not always sufficient for optimum correlation of features in secondary ion and optical images. On the other hand, a small collection of particles, such as those contained in the box in Figure 2a, can provide high confidence for pattern recognition and will be least likely to return false positive recognition results.

The program searches for each pattern in subsequent images captured by the frame grabber. If the pattern is not found in the normal mode of operation, the captured digital image is automatically modified by successive magnification and rotation adjustments. After each adjustment, the pattern recognition process is repeated. The scale and angle correction for the best match to the pattern is stored and displayed after the program has performed all specified permutations of the optical image.

Figure 3 illustrates the result of allowing the software to scale and rotate the image in Figure 2b until it finds the best correlation with the image in Figure 2a. The entire process of scaling, rotating, and pattern recognition required ~20 s (<1 to ~2 s/step) for the current system for 640 × 480 pixel images, but in general, the time required depends on the complexity of the pattern **F**. The quality of the pattern match is displayed at each scale/rotation step, and the best match is saved. After all iterations, the "corrected" image exhibiting the best feature-pattern match is displayed in the main image box, and the "found" pattern is outlined. Closer inspection of the matched feature and pattern in a separate window allows the user to accept or decline the computer match.

The record of the image processing performed permits correction for displacement, rotation, etc. if the sample remains on the microscope stage. For example, were a match found at a rotation of 30°, then the sample could be rotated by 30°, and a

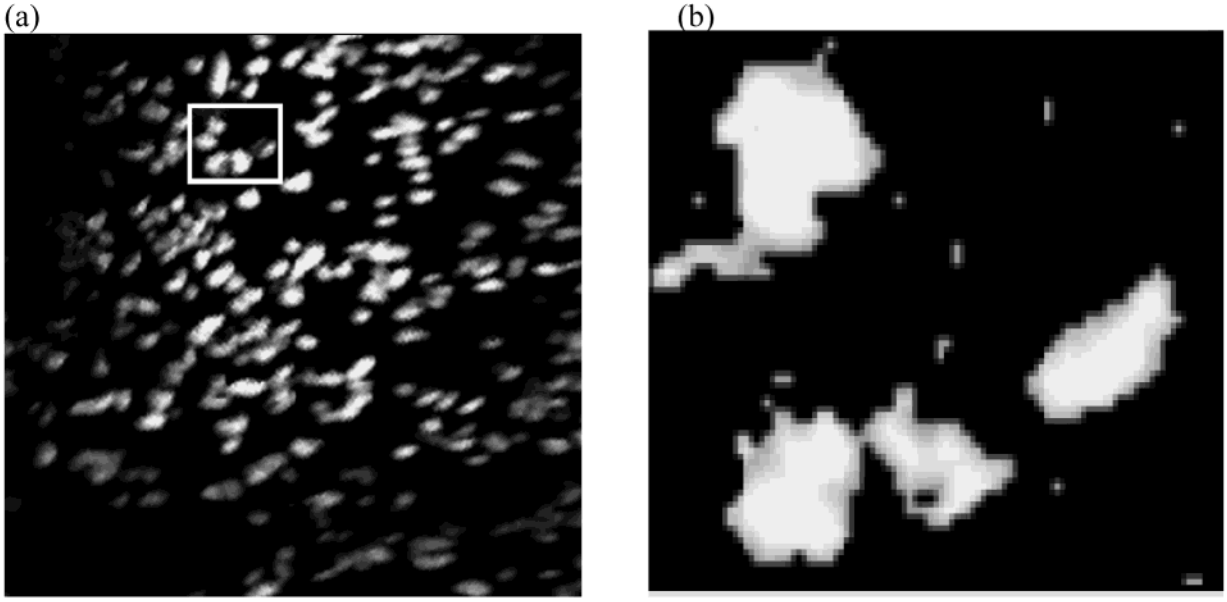

Figure 5. Secondary ion image (*m*/*z* 55, Mn) after translating the sample is shown as the large image. A magnified view of the defined pattern derived from thresholding the *m*/*z* 107 image shown in Figure 4 is shown in part b. Despite the fact that the defined pattern is much sharper than the corresponding match of the Mn image, a correct orientation can be ascertained by close inspection of the Mn image and the complementary Ag image.

subsequent image would be captured of the rotated sample. Similar manual manipulations could be used to reproduce magnification and illumination apparent in the reference image. After each manual change to the sample, a new correlation can be found. This can be done in real time with the frame grabber operating at ~1−5 frames/s and the "quality" of the correlation being presented each time the frame grabber is updated. In short, the sample can be manipulated until the image obtained via the frame grabber exactly matches the reference image.

One application of this capability is to determine the accurate "real world" position of some feature evident on the reference image, so that it could, for example, be excised for more detailed analysis by other methods. The location of the center of the feature space **F** is defined by its location in the reference image, that is, its pixel location, just as the center of the subset **P′** of the pattern space that best matches **F** is indicated. The pixel location could be transformed to real-world coordinates using calibration files that are stored for the camera/microscope. Calibration files are images of well-defined grids (high magnification) and precision-machined objects (lower magnification) that then define the geometric features in the image with real-world coordinates. Thus, definition of a unique pattern can be used to correct for geometric differences in two images and to calibrate the microscope/camera system to real-world coordinates.

Secondary Ion Image Correlation. Knowledge of the specific details of the secondary ion mass spectrometry used to create respective images is crucial to correlation of secondary ion images. For example, the sample shown in Figures 2 and 3 has a silver background. In itself, the secondary ion *m*/*z* 107 image is uninteresting, but the digitally inverted image of *m*/*z* 107 yields information about the distribution of all particles that are *not* silver. Digital image inversion means that at each pixel, the gray scale is indicated by $255-Ag^{+}_{normalized}$. We use double underline to indicate an inverted intensity image; e.g., Ag or m/z 107 is read as "not Ag" or "not *m*/*z* 107". Despite the clumsy nomenclature,

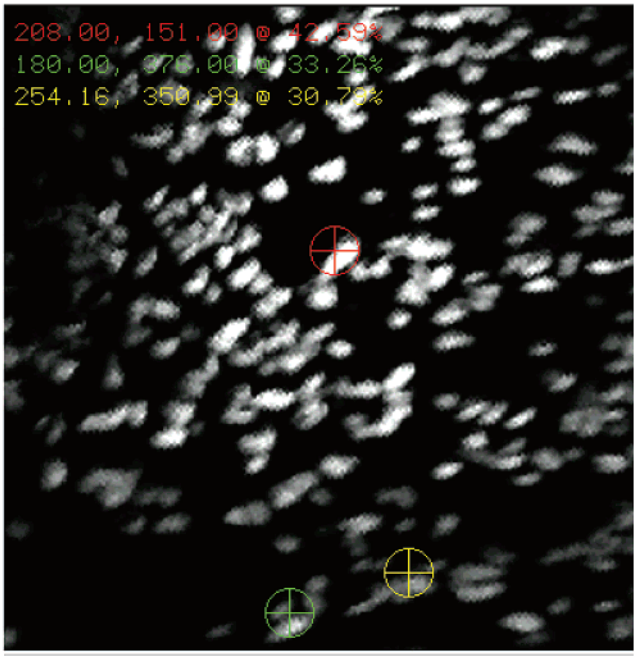

Figure 6. Search results from searching for similar patterns – providing position and rotation information for each result. The quality of fit is indicated by a normalized RMS difference between the pattern in the feature space and the selected region of the image or pattern space. Here, the three best fits are ranked red (42.6), green (33.3) and yellow (30.8), with the parenthetical numbers representing the normalized difference and 100 corresponding to a perfect fit. For images generated by a variety of different digital image processes, a perfect 100 is generally unlikely.

the advantage of the simple manipulation is evident in Figure 4. The m/z 107 secondary ion image displays features similar to the optical images of the same sample shown in Figure 2. The bright areas correspond to weak or no secondary ion emission of *m*/*z* 107 ions, and the dark areas correspond to strong emission. Thus,

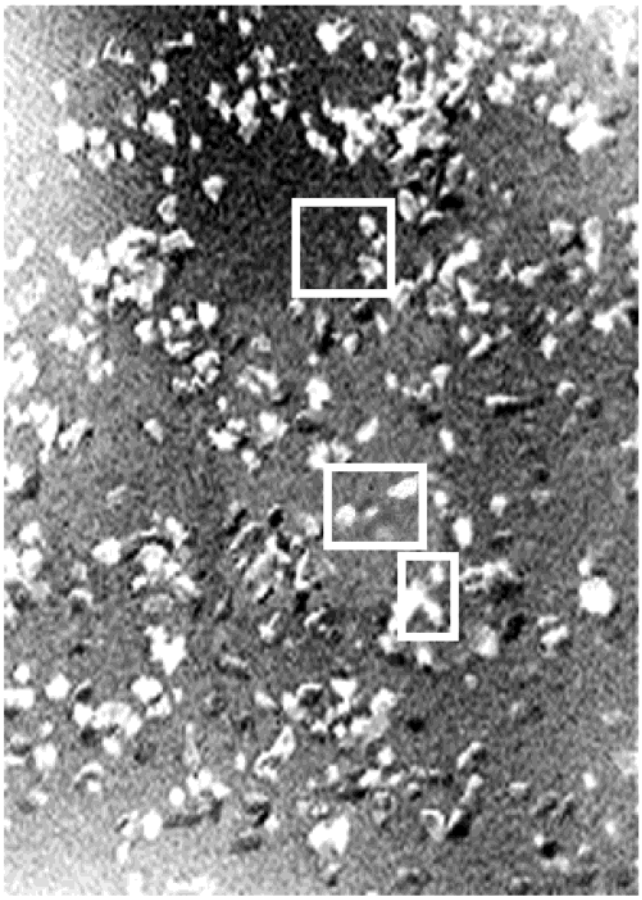

Figure 7. Secondary ion image (m/z 107) after correction for angle of incidence of primary ion gun ($y \times 2^{1/2}$). Three patterns defined for searching are outlined with white boxes.

the bright areas in the inverted secondary ion image correspond to the collection of Mn, Ti, and Pd particles dispersed over the silver substrate. Inversion of the m/z 107 intensity allows for correlation between the areas of low m/z 107 emission and ion images generated from the other constituents on the sample, for example the m/z 55 (Mn) ion image shown in Figures 5 and 6. To test the ability of the program to correlate secondary ion images, the sample was repositioned between obtaining the m/z 107 (Ag) and m/z 55 (Mn) secondary ion images.

The textured surface of the silver substrate generates variations in secondary ion emission that do not appear in the secondary ion emission from the dispersed metallic particles. For example, when set to transmit m/z 55, no signal at all is detected from the silver substrate, but variations in the Ag surface create fluctuations in secondary ion emission, clearly evident in the $\underline{\underline{Ag^+}}$ image. To compensate for this effect, it is necessary to perform a threshold operation on the $\underline{\underline{Ag^+}}$ image. Here, we use a 50% threshold; i.e., all inverted intensity below 128 is set to 0. The effect of this thresholding operation can be seen by comparing a magnified image the feature space shown in Figure 5b with the image in the white box of Figure 4; the granular background of the image is removed. Correlation between feature space taken from the $\underline{\underline{m/z\ 107}}$ image and a similar subset of the m/z 55 image (pattern space) was performed twice using the feature spaces defined in Figure 4. The best correlation is observed for a difference in scale (0.95) for Mn^+ and $\underline{\underline{Ag^+}}$ images, even though the images were

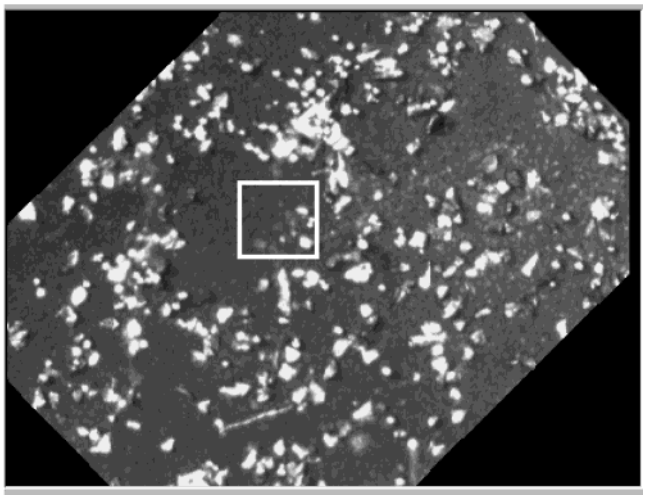

Figure 8. Rotation and scaling search for the best fit to the uppermost pattern of Figure 7 indicate −44.7° (counterclockwise) rotation and 0.64 magnification correction for the sample and microscope, respectively. When presented in almost real time, this information permits adjustments to the video capture of the sample image so that after some adjustment, the optical image of the sample can be readily compared to the secondary ion image.

obtained under identical secondary ion source conditions. The discrepancy in scale is likely a consequence of applying a threshold operation to the $\underline{\underline{^{107}Ag^+}}$ image. A small portion of the sample emits both Mn^+ and $\underline{\underline{Ag^+}}$, that is, at the boundary of any Mn flake. In the $\underline{\underline{Ag^+}}$ image (Figure 4), these pixels are set to zero, because their m/z 107 emission is below threshold; in contrast, no threshold operation was performed on the Mn^+ image. The positions of the two matched patterns were both shifted by the same x and y magnitudes when compared to the position of their corresponding defined feature spaces in Figure 4. Nearly identical shifts in relative position necessary for best correlation indicate that, although the apparent scale of the defined pattern is altered slightly as a result of partial subtraction of features, the scale of the overall image and relative positions of features have not changed.

Figure 6 shows the search results for the second feature space selected from the image in Figure 4. The score indicated in Figure 6 is a proprietary presentation of normalized variance between feature space and the subset of pattern space yielding the best fit. A score of 100 is defined as an exact match; a score of 0 is the score that would be obtained in comparison of feature space and a null space. The best correlation of three is indicated in the top right box of Figure 6, and the second and third best matches are also determined, allowing for comparison (by the user) of the similar individual patterns. The clear lack of fit, despite the mathematical evaluation, reflects the fact that the bright spots shown in Figure 4 indicate the position of all of the Mn, Pd, and Ti particles, whereas the bright spots of Figure 6 correspond to Mn only.

Secondary Ion Image to Optical Image Correlation. The overwhelming advantage that accrues to optical microscopy is that it can be performed at ambient pressure, whereas samples must be under high vacuum for analysis by SIMS. Therefore, for the purposes of correlation, the secondary ion images were loaded as reference files, and the optical image was obtained using the frame-grabber attached to a microscope system. This approach

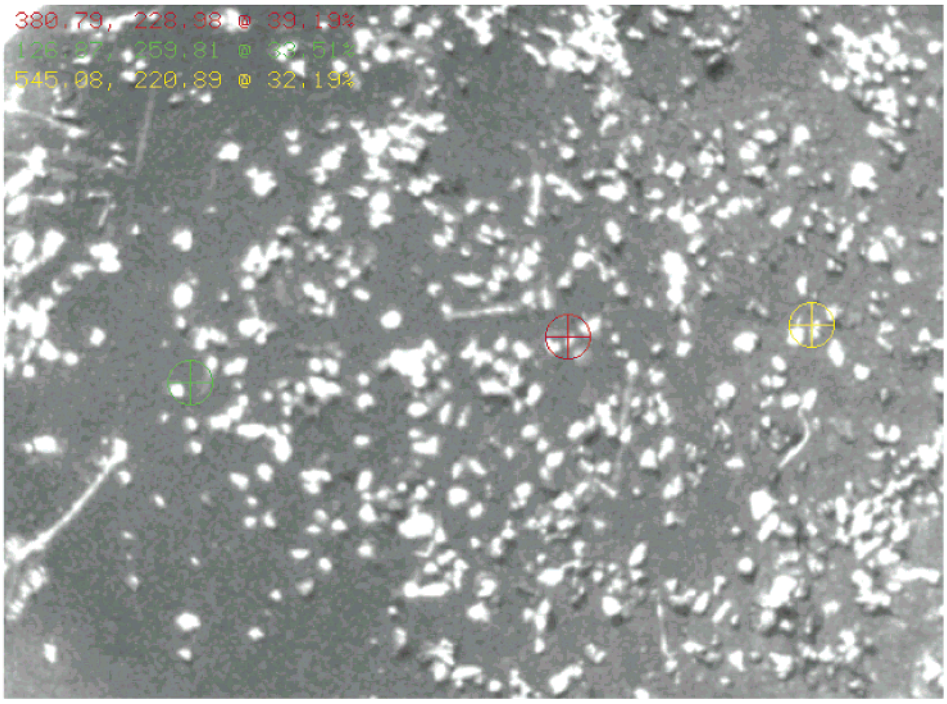

Figure 9. Search results for middle selected feature space pattern from Figure 7 after correction of sample rotation and camera magnification. The best fit (and correct correlation) is indicated by the red crosshairs, although inspection of the pattern in the vicinity of the yellow and green crosshairs yields some sense of the reason they were selected.

permits the sample and microscope to be adjusted to "zero" the sample after magnification and rotation are determined.

After normalization to bitmap format, correction must be made for effects of known geometric differences between the optical microscope and the ion microprobe. With the microprobe used here, the primary ion beam is aligned vertically 45° from the sample normal. As such, the digital raster, after identical amplification for both vertical and horizontal primary ion beam deflection, yields vertical deflection ~1.4× the horizontal deflection. The micrograph produced must be corrected for this effect. Figure 7 shows the resulting digital image after performing a nominal geometric correction on the $\underline{\underline{m/z\ 107}}$ image to compensate for vertical compression. Three feature spaces are defined on this (reference) ion image, outlined by white boxes. Again, these features were chosen for their lack of symmetry components. The top feature space contains three large particles nearly in a straight line, but it also has a large area that contains no other particles, which is unique in this large field of densely distributed particles. The other defined feature spaces are unique and distinguishable in an optical image. In some cases, feature spaces defined in the secondary ion image could not be correlated with any pattern in the optical image (pattern space). The failure of correlation with some feature spaces chosen reinforces the difficulty faced in image correlation across imaging platforms.

The next step of correlation is to find the magnification and rotation correction factors. Figure 8 shows the result of searching for the top feature space defined in the geometry-corrected $\underline{\underline{m/z\ 107}}$ image (Figure 7). Using the magnification and rotation factor determined by the best correlation, the microscope and sample positions are adjusted such that the secondary ion and optical images appear identical on the monitor. We found that this could be accomplished with the frame-grabber operating at ~1−4 frames/s simply by moving the sample slightly and adjusting the microscope. At this frame grabber rate, image processing must be minimal and small, and simple feature spaces must be used for recognition; however, more complicated correlations can be performed as necessary.

Figure 9 shows the search results for the second pattern (middle box from Figure 7) after correction for magnification and rotation has been performed. The matched pattern is marked by a crosshair marking the center of the best match between feature and pattern space; this position was stored for reference. As explained above, the three best pattern matches are determined and stored after each correlation attempt. Correlation was repeated in the same manner for the remaining feature spaces shown in Figure 7. Figure 10 highlights the three matched patterns on a calibrated optical image, which was cropped to resemble the geometry-corrected $\underline{\underline{m/z\ 107}}$ micrograph (Figure 7). The nominal image geometry correction performed does not completely compensate for the vertical compression evident in the secondary ion image shown in Figure 7. However, the position of the feature spaces in Figure 7 and the determined positions of the matched patterns in Figure 10 can be used to make "fine" corrections. This allows for precise coordinate transformation such that a pixel in one image (e.g., ion image) can be directly (and linearly) transformed to a pixel position in another image (e.g., optical image), and its respective position can be determined.

Registering the Optical Position of Pd Spheres. Perhaps the single most important goal of this research is to demonstrate identification and location of specific chemical species for subsequent excision, microanalysis, or both. Somewhere in the images shown in Figures 2−4 and 7−10 are 5 bright spots corresponding to 5 Pd spheres placed on the sample in an approximately straight line. These spheres can be readily distinguished by their second-

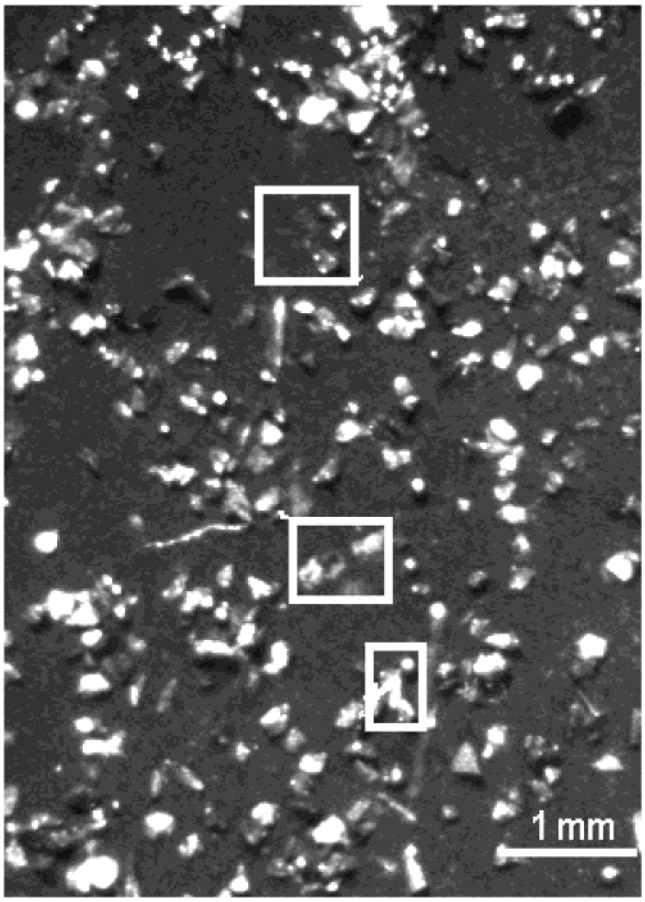

Figure 10. Correlated patterns in the optical image (outlined in white boxes), indicate an astigmatism in the secondary ion microprobe. However, all three defined patterns were found, and optical position data can be extracted from each pattern.

ary ion (m/z 106) emission, as shown in the right-hand figure of Figure 11.

Although the ion micrograph provides information about the relative distribution of the spheres in a vacuum, information more useful to us is the exact location of the spheres as they sit on a microscope stage at atmosphere. Thus, it is necessary to determine the position of the palladium spheres in the optical image (using the first-order fits determined by the m/z 107 image). This method would ultimately provide the most reliable results for coordinate transforms.

As demonstrated above, correlation of image data across platforms does not yield an exact fit. This begs the question that if image A correlates with image B and image B correlates with image C, does image A correlate with image C? Moreover, can the machine vision algorithms of SIMSearch make a valid correlation? This is more than an academic question. Such circumstances arise when three or more imaging methods are employed or when it is necessary to analyze the same sample under different instrumental conditions, on different days, in different positions, etc. So-called round-robin analyses are a good example.

These questions can be answered with the data in hand when combined with the secondary Pd^+ image shown in the right-hand side of Figure 11. Except for the transmitted secondary ion, this image was obtained under the same conditions as the Mn^+ image shown in Figure 5. Therefore, the pixel coordinates of the Pd image correspond to those in the Mn image directly. As shown above, the Mn^+ image correlates with the Ag^+ image, which in turn is correlated with the optical image. Thus, any coordinate in the Pd^+ image can be transformed to a position on the optical image. After all coordinate transformation factors have been determined (i.e., from both image shift and the correlation between ion and optical images), the program allows a point or a number of points to be selected from one image and then displayed as the corresponding points on the other image. Figure 11 shows the screen capture from picking the five Pd spheres in the m/z 106 (Pd) image (right window image) and the screen capture showing the position of the five palladium spheres in the optical image (left window image). The relative spacing of the

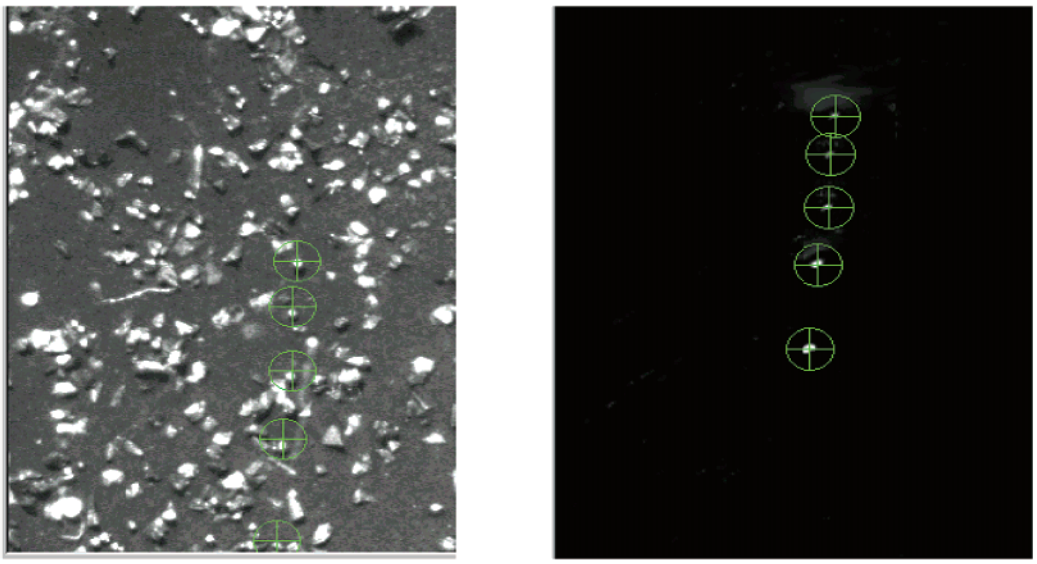

Figure 11. Cropped portion of (a) optical image and (b) secondary ion image of Pd^+ (m/z 106) obtained from the sample containing 5 Pd spheres arrayed in an approximately straight line and mixed with Mn flakes and Ti spheres on a Ag substrate. Once two images are correlating, selecting points on the secondary ion by computer permits selection of corresponding points on the optical image. This allows the otherwise indistinguishable Pd spheres to be identified on the optical image.

cross-hairs indicates that application of successive coordinate transforms is appropriate.

CONCLUSION

The program we have developed, entitled SIMSearch, has been applied to correlating secondary ion and optical images. The operations performed on the images are purely mathematical and, thus, should be applicable to images of the same sample, regardless of their origin. The algorithms integrated into SIMSearch do not depend on the type of method used to obtain an image. The fact that the program permits automated correlation of images and then yields appropriate coordinates for subsequent operations implies that the tedium associated with image correlation and particle excision can be substantially reduced.

Although we have not addressed the issue, application of SIMSearch to complementary methods may yield results that are greater than the sum of the data. Analytical images are almost always obtained with the purpose of determining correspondence between at least two chemical or physical features. However, it frequently happens that only one feature is apparent with a particular type of image, and another analytical method must be used to display the complementary feature. This type of problem can be accommodated by application of chemical knowledge to the mathematical operations of pattern recognition. For example, given that an Mn^+ secondary ion image and an optical image correlated, we could determine the location of Pd spheres evidenced in an optical image by knowing the position of the spheres relative to Mn flakes apparent in a secondary ion image. This, of course, is a trivial example, but it is not difficult to imagine determining the location of trace contaminants evident in a secondary ion image relative to features evident in optical, SEM, or scanning probe image. In summary, we see application of SIMSearch as a potential method to combine data from the two methods in an automated and reliable way.

ACKNOWLEDGMENT

This research was sponsored by the Division of Chemical Sciences, Geosciences, and Biosciences, Office of Basic Energy Sciences, U.S. Department of Energy, and by the Office of Nuclear Nonproliferation (NN-44), U. S. Department of Energy. Oak Ridge National Laboratory is managed and operated by UT-Battelle, LLC, for the U.S. Department of Energy under contract DE-AC05-00OR22725.

Received for review April 9, 2002. Accepted June 24, 2002.

AC025693B